curves were constructed using the Kaplan–Meier method and compared with the log-rank test. The analyses were carried out using the JMP 7 statistics package (SAS Institute, Cary, NC, USA). Multivariate analysis was evaluated by Cox's proportional hazards model.

Conclusion

We comprehensively analyzed genomic alterations in endometrial carcinomas. The novel classification by the number of chromosomal imbalances revealed that CIN-extensive is an independent poor prognostic factor. As the status of genomic instability is not morphologically recognized, our CIN classification would provide a useful biomarker for prognosis in endometrial carcinomas. SNP array analysis revealed CNN LOH at 42% and HD at 10%, including the locus of *PTEN*. Our data indicated that alterations in the Ras-PI3K pathway are extensively prevalent in endometrial carcinomas through both chromosomal imbalances and genetic mutations.

Conflict of interest

The authors declare no conflict of interest.

Acknowledgements

We thank Hiroko Meguro, Akira Watanabe, Jennifer Okada, Toshiharu Yasugi, Kei Kawana, Takahide Arimoto, Akira Tsuchiya, Osamu Hiraike-Wada, Kenbun Sone, Yuichiro Miyamoto, Haruko Hiraike, Katsuyuki Adachi, Shiho Miura and Ayako Tomio for support and assistance. This work was supported by the Ministry of Education, Science, Sports and Culture Grant Number: Scientific Research (S) 16101006, Scientific Research on Priority Areas 17015008, Ministry of Education, Culture, Sports, Science and Technology of Japan on Priority Area; Grant Number: 20014007, and Core Research for Evolutional Science and Technology (CREST), Japan Science and Technology Agency (JST) (to H Aburatani); by the Grant-in-Aid for Scientific Research (C), Grant Number 19599005 and the Grant-in-Aid for Young Scientists (B), Grant Number 21791544 from the Ministry of Education, Culture, Sports, Science and Technology of Japan (to K Oda); by the Grant-in-Aid for Scientific Research on Priority Areas 'Applied Genomics', Grant Number 20018005, from the Ministry of Education, Culture, Sports, Science and Technology of Japan and Industrial Technology Research Grant Program from New Energy and Industrial Technology Development Organization (NEDO) of Japan (to S Ishikawa).

References

An HJ, Logani S, Isacson C, Ellenson LH. (2004). Molecular characterization of uterine clear cell carcinoma. *Mod Pathol* **17**: 530–537.

Arabi H, Guan H, Kumar S, Cote M, Bandyopadhyay S, Shah J *et al.* (2009). Impact of microsatellite instability (MSI) on survival in high grade endometrial carcinoma. *Gynecol Oncol* **113**: 153–158.

Atkin NB. (2001). Microsatellite instability. *Cytogenet Cell Genet* **92**: 177–181.

Bacolod MD, Schemmann GS, Giardina SF, Paty P, Notterman DA, Barany F. (2009). Emerging paradigms in cancer genetics: some important findings from high-density single nucleotide polymorphism array studies. *Cancer Res* **69**: 723–727.

Bilbao C, Rodríguez G, Ramírez R, Falcón O, León L, Chirino R *et al.* (2006). The relationship between microsatellite instability and PTEN gene mutations in endometrial cancer. *Int J Cancer* **119**: 563–570.

Black D, Soslow RA, Levine DA, Tornos C, Chen SC, Hummer AJ *et al.* (2006). Clinicopathologic significance of defective DNA mismatch repair in endometrial carcinoma. *J Clin Oncol* **24**: 1745–1753.

Cancer Genome Atlas Research Network (2008). Comprehensive genomic characterization defines human glioblastoma genes and core pathways. *Nature* **455**: 1061–1068.

Carpten JD, Faber AL, Horn C, Donoho GP, Briggs SL, Robbins CM *et al.* (2007). A transforming mutation in the pleckstrin homology domain of AKT1 in cancer. *Nature* **448**: 439–444.

Cheng JQ, Godwin AK, Bellacosa A, Taguchi T, Franke TF, Hamilton TC *et al.* (1992). AKT2, a putative oncogene encoding a member of a subfamily of protein-serine/threonine kinases, is amplified in human ovarian carcinomas. *Proc Natl Acad Sci USA* **89**: 9267–9271.

Choi SW, Lee KJ, Bae YA, Min KO, Kwon MS, Kim KM *et al.* (2002). Genetic classification of colorectal cancer based on chromosomal loss and microsatellite instability predicts survival. *Clin Cancer Res* **8**: 2311–2322.

Conrad DF, Andrews TD, Carter NP, Hurles ME, Pritchard JK. (2006). A high-resolution survey of deletion polymorphism in the human genome. *Nat Genet* **38**: 75–81.

Doll A, Abal M, Rigau M, Monge M, Gonzalez M, Demajo S *et al.* (2008). Novel molecular profiles of endometrial cancer-new light through old windows. *J Steroid Biochem Mol Biol* **108**: 221–229.

Dunbar AJ, Gondek LP, O'Keefe CL, Makishima H, Rataul MS, Szpurka H *et al.* (2008). 250K single nucleotide polymorphism array karyotyping identifies acquired uniparental disomy and homozygous mutations, including novel missense substitutions of c-Cbl, in myeloid malignancies. *Cancer Res* **68**: 10349–10357.

Enomoto T, Inoue M, Perantoni AO, Buzard GS, Miki H, Tanizawa O *et al.* (1991). K-ras activation in premalignant and malignant epithelial lesions of the human uterus. *Cancer Res* **51**: 5308–5314.

Fitzgibbon J, Smith LL, Raghavan M, Smith ML, Debernardi S, Skoulakis S *et al.* (2005). Association between acquired uniparental disomy and homozygous gene mutation in acute myeloid leukemias. *Cancer Res* **65**: 9152–9154.

Flotho C, Steinemann D, Mullighan CG, Neale G, Mayer K, Kratz CP *et al.* (2007). Genome-wide single-nucleotide polymorphism analysis in juvenile myelomonocytic leukemia identifies uniparental disomy surrounding the NF1 locus in cases associated with neurofibromatosis but not in cases with mutant RAS or PTPN11. *Oncogene* **26**: 5816–5821.

Geigl JB, Obenauf AC, Schwarzbraun T, Speicher MR. (2008). Defining 'chromosomal instability'. *Trends Genet* **24**: 64–69.

Gorringe KL, Campbell IG. (2008). High-resolution copy number arrays in cancer and the problem of normal genome copy number variation. *Genes Chromosomes Cancer* **47**: 933–938.

Gorringe KL, Jacobs S, Thompson ER, Sridhar A, Qiu W, Choong DY *et al.* (2007). High-resolution single nucleotide polymorphism array analysis of epithelial ovarian cancer reveals numerous microdeletions and amplifications. *Clin Cancer Res* **13**: 4731–4739.

Gorringe KL, Ramakrishna M, Williams LH, Sridhar A, Boyle SE, Bearfoot JL *et al.* (2009). Are there any more ovarian tumor suppressor genes? A new perspective using ultra high-resolution copy number and loss of heterozygosity analysis. *Genes Chromosomes Cancer* **48**: 931–942.

Grady WM. (2004). Genomic instability and colon cancer. *Cancer Metastasis Rev* **23**: 11–27.

Hirasawa A, Aoki D, Inoue J, Imoto I, Susumu N, Sugano K *et al.* (2003). Unfavorable prognostic factors associated with high frequency of microsatellite instability and comparative genomic hybridization analysis in endometrial cancer. *Clin Cancer Res* **9**: 5675–5682.

Ishikawa S, Komura D, Tsuji S, Nishimura K, Yamamoto S, Panda B *et al.* (2005). Allelic dosage analysis with genotyping microarrays. *Biochem Biophys Res Commun* **333**: 1309–1314.

Kawamata N, Ogawa S, Zimmermann M, Kato M, Sanada M, Hemminki K *et al.* (2008). Molecular allelokaryotyping of pediatric acute lymphoblastic leukemias by high-resolution single nucleotide polymorphism oligonucleotide genomic microarray. *Blood* **111**: 776–784.

Komura D, Shen F, Ishikawa S, Fitch KR, Chen W, Zhang J *et al.* (2006). Genome-wide detection of human copy number variations using high-density DNA oligonucleotide arrays. *Genome Res* **16**: 1575–1584.

Kong D, Suzuki A, Zou TT, Sakurada A, Kemp LW, Wakatsuki S *et al.* (1997). PTEN1 is frequently mutated in primary endometrial carcinomas. *Nat Genet* **17**: 143–144.

Kong D, Yamori T. (2008). Phosphatidylinositol 3-kinase inhibitors: promising drug candidates for cancer therapy. *Cancer Sci* **99**: 1734–1740.

Kralovics R, Passamonti F, Buser AS, Teo SS, Tiedt R, Passweg JR *et al.* (2005). A gain-of-function mutation of JAK2 in myeloproliferative disorders. *N Engl J Med* **352**: 1779–1790.

Kratz CP, Steinemann D, Niemeyer CM, Schlegelberger B, Koscielniak E, Kontny U *et al.* (2007). Uniparental disomy at chromosome 11p15.5 followed by HRAS mutations in embryonal rhabdomyosarcoma: lessons from Costello syndrome. *Hum Mol Genet* **16**: 374–379.

Levan K, Partheen K, Osterberg L, Helou K, Horvath G. (2006). Chromosomal alterations in 98 endometrioid adenocarcinomas analyzed with comparative genomic hybridization. *Cytogenet Genome Res* **115**: 16–22.

Li J, Yen C, Liaw D, Podsypanina K, Bose S, Wang SI *et al.* (1997). PTEN, a putative protein tyrosine phosphatase gene mutated in human brain, breast, and prostate cancer. *Science* **275**: 1943–1947.

Loukola A, Eklin K, Laiho P, Salovaara R, Kristo P, Jarvinen H *et al.* (2001). Microsatellite marker analysis in screening for hereditary nonpolyposis colorectal cancer (HNPCC). *Cancer Res* **61**: 4545–4549.

Lynch TJ, Bell DW, Sordella R, Gurubhagavatula S, Okimoto RA, Brannigan BW *et al.* (2004). Activating mutations in the epidermal growth factor receptor underlying responsiveness of non-small-cell lung cancer to gefitinib. *N Engl J Med* **350**: 2129–2139.

Maira SM, Stauffer F, Schnell C, Garcia Echeverria C. (2009). PI3K inhibitors for cancer treatment: where do we stand? *Biochem Soc Trans* **37**: 265–272.

McCormick F. (1995). Ras signaling and NF1. *Curr Opin Genet Dev* **5**: 51–55.

Melcher R, Al Taie O, Kudlich T, Hartmann E, Maisch S, Steinlein C *et al.* (2007). SNP-Array genotyping and spectral karyotyping reveal uniparental disomy as early mutational event in MSS- and MSI-colorectal cancer cell lines. *Cytogenet Genome Res* **118**: 214–221.

Micci F, Teixeira MR, Haugom L, Kristensen G, Abeler VM, Heim S. (2004). Genomic aberrations in carcinomas of the uterine corpus. *Genes Chromosomes Cancer* **40**: 229–246.

Midorikawa Y, Yamamoto S, Ishikawa S, Kamimura N, Igarashi H, Sugimura H *et al.* (2006). Molecular karyotyping of human hepatocellular carcinoma using single-nucleotide polymorphism arrays. *Oncogene* **25**: 5581–5590.

Minaguchi T, Yoshikawa H, Oda K, Ishino T, Yasugi T, Onda T *et al.* (2001). PTEN mutation located only outside exons 5, 6, and 7 is an independent predictor of favorable survival in endometrial carcinomas. *Clin Cancer Res* **7**: 2636–2642.

Oda K, Okada J, Timmerman L, Rodriguez Viciana P, Stokoe D, Shoji K *et al.* (2008). PIK3CA cooperates with other phosphatidylinositol 3′-kinase pathway mutations to effect oncogenic transformation. *Cancer Res* **68**: 8127–8136.

Oda K, Stokoe D, Taketani Y, McCormick F. (2005). High frequency of coexistent mutations of PIK3CA and PTEN genes in endometrial carcinoma. *Cancer Res* **65**: 10669–10673.

Onda T, Yoshikawa H, Mizutani K, Mishima M, Yokota H, Nagano H *et al.* (1997). Treatment of node-positive endometrial cancer with complete node dissection, chemotherapy and radiation therapy. *Br J Cancer* **75**: 1836–1841.

Parkin DM. (2001). Global cancer statistics in the year 2000. *Lancet Oncol* **2**: 533–543.

Raghavan M, Lillington DM, Skoulakis S, Debernardi S, Chaplin T, Foot NJ *et al.* (2005). Genome-wide single nucleotide polymorphism analysis reveals frequent partial uniparental disomy due to somatic recombination in acute myeloid leukemias. *Cancer Res* **65**: 375–378.

Rowan A, Halford S, Gaasenbeek M, Kemp Z, Sieber O, Volikos E *et al.* (2005). Refining molecular analysis in the pathways of colorectal carcinogenesis. *Clin Gastroenterol Hepatol* **3**: 1115–1123.

Ryan AJ, Susil B, Jobling TW, Oehler MK. (2005). Endometrial cancer. *Cell Tissue Res* **322**: 53–61.

Salvesen HB, Carter SL, Mannelqvist M, Dutt A, Getz G, Stefansson IM *et al.* (2009). Integrated genomic profiling of endometrial carcinoma associates aggressive tumors with indicators of PI3 kinase activation. *Proc Natl Acad Sci USA* **106**: 4834–4839.

Samuels Y, Wang Z, Bardelli A, Silliman N, Ptak J, Szabo S *et al.* (2004). High frequency of mutations of the PIK3CA gene in human cancers. *Science* **304**: 554.

Shayesteh L, Lu Y, Kuo WL, Baldocchi R, Godfrey T, Collins C *et al.* (1999). PIK3CA is implicated as an oncogene in ovarian cancer. *Nat Genet* **21**: 99–102.

Shoji K, Oda K, Nakagawa S, Hosokawa S, Nagae G, Uehara Y *et al.* (2009). The oncogenic mutation in the pleckstrin homology domain of AKT1 in endometrial carcinomas. *Br J Cancer* **101**: 145–148.

Sirchia SM, Sironi E, Grati FR, Serafini P, Garagiola I, Rossella F *et al.* (2000). Losses of heterozygosity in endometrial adenocarcinomas: positive correlations with histopathological parameters. *Cancer Genet Cytogenet* **121**: 156–162.

Slamon DJ, Godolphin W, Jones LA, Holt JA, Wong SG, Keith DE *et al.* (1989). Studies of the HER-2/neu proto-oncogene in human breast and ovarian cancer. *Science* **244**: 707–712.

Stokoe D, Stephens LR, Copeland T, Gaffney PR, Reese CB, Painter GF *et al.* (1997). Dual role of phosphatidylinositol-3,4,5-trisphosphate in the activation of protein kinase B. *Science* **277**: 567–570.

Suehiro Y, Umayahara K, Ogata H, Numa F, Yamashita Y, Oga A *et al.* (2000). Genetic aberrations detected by comparative genomic hybridization predict outcome in patients with endometrioid carcinoma. *Genes Chromosomes Cancer* **29**: 75–82.

Tashiro H, Lax SF, Gaudin PB, Isacson C, Cho KR, Hedrick L. (1997). Microsatellite instability is uncommon in uterine serous carcinoma. *Am J Pathol* **150**: 75–79.

Teh MT, Blaydon D, Chaplin T, Foot NJ, Skoulakis S, Raghavan M *et al.* (2005). Genomewide single nucleotide polymorphism microarray mapping in basal cell carcinomas unveils uniparental disomy as a key somatic event. *Cancer Res* **65**: 8597–8603.

Toda T, Oku H, Khaskhely NM, Moromizato H, Ono I, Murata T. (2001). Analysis of microsatellite instability and loss of heterozygosity in uterine endometrial adenocarcinoma. *Cancer Genet Cytogenet* **126**: 120–127.

Tuna M, Knuutila S, Mills GB. (2009). Uniparental disomy in cancer. *Trends Mol Med* **15**: 120–128.

Vogelstein B, Fearon ER, Hamilton SR, Kern SE, Preisinger AC, Leppert M *et al.* (1988). Genetic alterations during colorectal-tumor development. *N Engl J Med* **319**: 525–532.

Walsh CS, Ogawa S, Scoles DR, Miller CW, Kawamata N, Narod SA *et al.* (2008). Genome-wide loss of heterozygosity and uniparental disomy in BRCA1/2-associated ovarian carcinomas. *Clin Cancer Res* **14**: 7645–7651.

Weber JC, Meyer N, Pencreach E, Schneider A, Guerin E, Neuville A *et al.* (2007). Allelotyping analyses of synchronous primary and metastasis CIN colon cancers identified different subtypes. *Int J Cancer* **120**: 524–532.

Woerner SM, Benner A, Sutter C, Schiller M, Yuan YP, Keller G *et al.* (2003). Pathogenesis of DNA repair-deficient cancers: a statistical meta-analysis of putative Real Common Target genes. *Oncogene* **22**: 2226–2235.

Supplementary Information accompanies the paper on the Oncogene website (http://www.nature.com/onc)

Cancer Science
The official journal of the Japanese Cancer Association JCA

Potent *in vitro* and *in vivo* antitumor effects of MDM2 inhibitor nutlin-3 in gastric cancer cells

Shinji Endo,[1] Kenji Yamato,[2] Sachiko Hirai,[1] Toshikazu Moriwaki,[1] Kuniaki Fukuda,[1] Hideo Suzuki,[1] Masato Abei,[1] Ichiro Nakagawa[2] and Ichinosuke Hyodo[1,3]

[1]Department of Gastroenterology and Hepatology, Institute of Clinical Medicine, Graduate School of Comprehensive Human Sciences, University of Tsukuba, Tsukuba; [2]Section of Bacterial Pathogenesis, Graduate School of Medical and Dental Science, Tokyo Medical and Dental University, Tokyo, Japan

(Received August 30, 2010/Revised November 29, 2010/Accepted December 1, 2010/Accepted manuscript online December 7, 2010)

The tumor suppressor gene *p53* is the most frequently mutated gene in human cancers. However, its mutation rate is relatively low in gastric cancer compared with other cancers. In this study, we investigated the mechanisms underlying the antitumor effects of nutlin-3, an inhibitor of human homolog of murine double minute 2 (MDM2). MDM2 is a negative regulator of p53. Four gastric cancer cell lines with wild-type *p53* (wt *p53*) and three with mutant-type *p53* (mt *p53*) were analyzed for MDM2 and MDM4 expression by immunoblotting, and for their gene amplification by quantitative real-time PCR. Moreover, the viability of cells exposed to nutlin-3 was examined by WST-8 assay, and the expression of p53 and its downstream genes was analyzed by immunoblotting. Nutlin-3 stabilized p53 and increased the expression of $p21^{WAF1}$ and Noxa, and cleaved poly (ADP)-ribose polymerase regardless of the pre-expression levels of MDM2 and MDM4 in gastric cancer cells with wt *p53*. Flow cytometry revealed that nutlin-3 arrested the cell cycle in G_1 phase and induced apoptosis in the cell lines. These nutlin-3 effects were not observed in the cell lines with mt *p53*. Nutlin-3 exerted additive or synergistic cytotoxicity in combination with 5-fluorouracil or cisplatin in most cell lines with wt *p53*. An *in vivo* antitumor effect of nutlin-3 alone and its additive augmentation by 5-fluorouracil were confirmed in an MDM2 overexpressed xenograft tumor model. Nutlin-3 showed potent antitumor activity against human gastric cancer cells with wt *p53* and shows promise as a single agent and in combination with conventional anticancer drugs. (*Cancer Sci*, doi: 10.1111/j.1349-7006.2010.01821.x, 2011)

The tumor suppressor gene *p53* plays a central role in the regulation of the cell cycle, DNA repair, apoptosis, and senescence.[1–3] Deleted or mutated p53 occurs in approximately half of human cancers, indicating that a substantial proportion of human carcinogenesis is caused by dysfunction of the p53 pathway.[4] In human gastric cancer, the rate of *p53* mutation is approximately 30%.[5,6] To date, the efficacy of p53 pathway activation in controlling gastric cancer with wild-type *p53* (wt *p53*) has not yet been fully elucidated.

Human homolog of murine double minute 2 (MDM2) negatively regulates p53.[7] MDM2 is a p53-specific E3 ubiquitin ligase that mediates the ubiquitin-dependent degradation of p53.[8,9] Moreover, MDM2 can bind to the p53 transactivation domain and suppress p53-mediated transcription.[10,11] *MDM2* expression is positively regulated by p53 transactivation, forming a feedback loop. Amplified *MDM2* has been observed in human sarcomas[9,12] and in >10% of various human cancers including gastric cancers.[13,14] MDM4 was discovered as a p53-binding protein negatively regulated by MDM2 and has structural homology with MDM2.[15] *MDM4* is also amplified or overexpressed in 10–20% of various human cancers[7,16] and 65% of retinoblastomas.[17] Unlike MDM2, MDM4 is neither activated by p53 nor has intrinsic ubiquitin-ligase activity. MDM4 regulates p53 activity by interacting with the p53 transactivation domain and thereby inhibiting p53-mediated gene expression.[18,19]

Nutlin-3 is a novel small-molecule inhibitor of MDM2.[20,21] It binds to MDM2 in the p53-binding pocket, interfering with MDM2-directed p53 degradation and resulting in p53 accumulation. Increased p53 activates p53-responsive genes involved in G_1 arrest and apoptosis. In addition, nutlin-3 exerts antitumor effects in solid tumors and lymphoid neoplasms with wt *p53*.[22–24] However, its *in vitro* and *in vivo* antitumor effects in gastric cancer cells have not yet been sufficiently clarified.

We analyzed various gastric cancer cell lines for the expression of MDM2 and MDM4 and their sensitivity to nutlin-3 with or without anticancer drugs. We also investigated the *in vivo* antitumor effects of nutlin-3 alone and its enhancement by 5-fluorouracil (5-FU) in a xenograft model of a human gastric cancer cell line with wt *p53*.

Materials and Methods

Cell lines. Seven gastric cancer cell lines were used: four cell lines with wt *p53* (MKN-45, NUGC-4, STKM-2, and SNU-1);[25–27] and three cell lines with mutant-type *p53* (mt *p53*; NUGC-3, NUGC-2, and STKM-1).[26] Cell lines with wt *p53* derived from other types of cancer (SJSA-1 osteosarcoma, MCF-7 breast cancer, and Weri-1 retinoblastoma cell lines) were also studied. MKN-45, NUGC-4, and Weri-1 cell lines were obtained from Riken BRC Cell Bank (Tsukuba, Japan). SNU-1, SJSA-1, and WI-38 (human diploid fibroblasts) cell lines were purchased from the American Type Culture Collection (Rockville, MD, USA). NUGC-3 and NUGC-2 cell lines were obtained from Health Science Research Resources Bank (Osaka, Japan). STKM-1 and STKM-2 cell lines were kindly provided by Dr. Shunsuke Yanoma (School of Medicine, Yokohama City University, Japan).

Chemicals. Nutlin-3 and 5-FU were purchased from Calbiochem (San Diego, CA, USA) and Wako (Osaka, Japan), respectively. Cisplatin (CDDP) was obtained from Toronto Research Chemicals (North York, ON, Canada). All reagents were used in different concentrations as indicated.

Immunoblot analysis. Both SDS-PAGE and Western blot analysis were carried out as previously described.[28] Primary and secondary antibodies used were as follows. Monoclonal antibodies against MDM2 (2A10), MDM4 (MDMX-82), $p21^{WAF1}$ (EA10), and Noxa (114C307) were purchased from Abcam (Cambridge, MA, USA). Anti-MDM4 (D-4) antibody was obtained from Santa Cruz Biotechnology (Santa Cruz, CA, USA). Anti-p53 mouse mAb (BP53-12) was purchased from

[3]To whom correspondence should be addressed.
E-mail: ihyodo@md.tsukuba.ac.jp

doi: 10.1111/j.1349-7006.2010.01821.x

Cell Sciences (Canton, MA, USA). Anti-p14^{ARF} (DCS-240) mouse monoclonal, ALP-conjugated goat anti-mouse IgG, and ALP-conjugated anti-rabbit IgG antibodies were obtained from Sigma-Aldrich (St. Louis, MI, USA). Rabbit anti-cleaved poly (ADP)-ribose polymerase (PARP; Asp214) and anti-β-actin mAbs were procured from Cell Signaling Technology (Danvers, MA, USA).

Real-time quantitative PCR analysis of *MDM2* and *MDM4* gene copy numbers. DNA samples were extracted from cell lysate using a QIAamp DNA mini kit (Qiagen, Germantown, MD, USA) according to the manufacturer's instructions. Real-time quantitative PCR was carried out using a Roche LightCycler 480 Real-Time PCR System (Roche Applied Science, Mannheim, Germany). Primers and TaqMan probe for *MDM2*, *MDM4*, and the reference gene of *MRPL19*[29] were obtained from Applied Biosystems (Foster City, CA, USA; Table 1). Reactions were carried out in triplicate under standard thermocycling conditions using 20 ng genomic DNA, 200 nM primers, 1 μM probes, and LightCycler 480 Probes Master (Roche Applied Science), according to the manufacturer's protocol.

DNA extracted from the cell lines and fibroblasts was analyzed for relative amount of the target gene (*MDM2*, *MDM4*) and reference gene (*MRPL19*) by quantitative real-time PCR. The relative copy number (Q) of *MDM2 versus MRPL19* was calculated using the following equation:[30]

Table 1. Polymerase chain reaction primers and TaqMan probes used in this study

Gene	Sequence
MDM2	
Forward primer	5′-CAGGACATCTTATGGCCTGCTT
Reverse primer	5′-GGGCAGGGCTTATTCCTTTT
Probe	5′-FAM-CATGTGCAAAGAAGCTA
MDM4	
Forward primer	5′-TCCCTGCAACTCAGTGGAATT
Reverse primer	5′-TGAGATGGTCTCTTGGCTTTCA
Probe	5′-FAM-TTGGATTTGGCTCACAGTT
MRPL19	
Forward primer	5′-GCTAAACAGAAGGCTCACCACAA
Reverse primer	5′-CACATTTCTGCAACATCCAG
Probe	5′-FAM-ATCTGGCAGGATTATACT

$$Q = qT/qN,$$

$$qT = V^{T}_{\text{target gene}} \Big/ V^{T}_{\text{reference gene}},$$

$$qN = V^{N}_{\text{target gene}} \Big/ V^{N}_{\text{reference gene}},$$

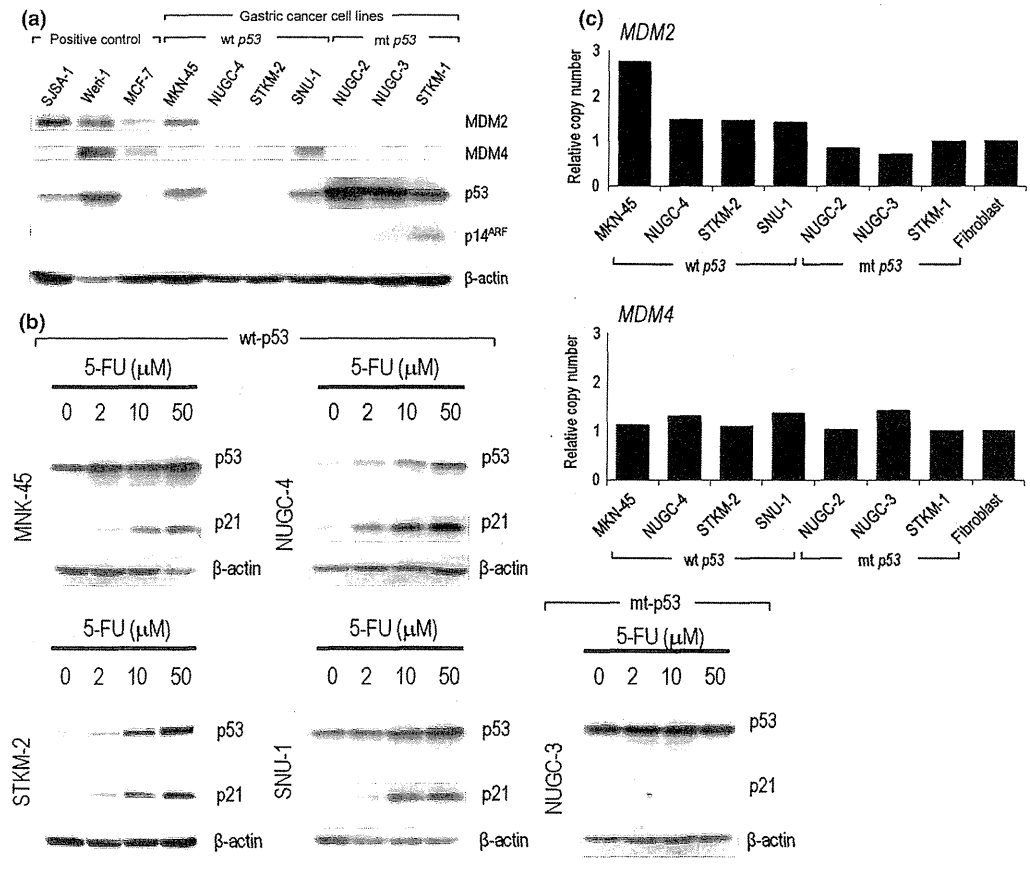

Fig. 1. Expression of human homolog of murine double minute 2 (MDM2), MDM4, and p53 in gastric cancer cells. (a) MDM2, MDM4, p53, and p14^{ARF} expression in seven gastric cancer cell lines was examined by immunoblotting. (b) Four cell lines with wild-type (wt) *p53* (MKN-45, NUGC-4, STKM-2, and SNU-1) and one cell line with mutant-type (mt) *p53* (NUGC-3) were exposed to various concentrations of 5-fluorouracil (5-FU) for 24 h and analyzed for p53 and p21^{WAF1} expression by immunoblotting. (c) DNA amplification of *MDM2* and *MDM4* in gastric cancer cells by quantitative real-time PCR. Copy numbers of *MDM2* and *MDM4* in gastric cancer cell lines were compared with those in fibroblasts using *MRPL19* as a reference gene.

doi: 10.1111/j.1349-7006.2010.01821.x

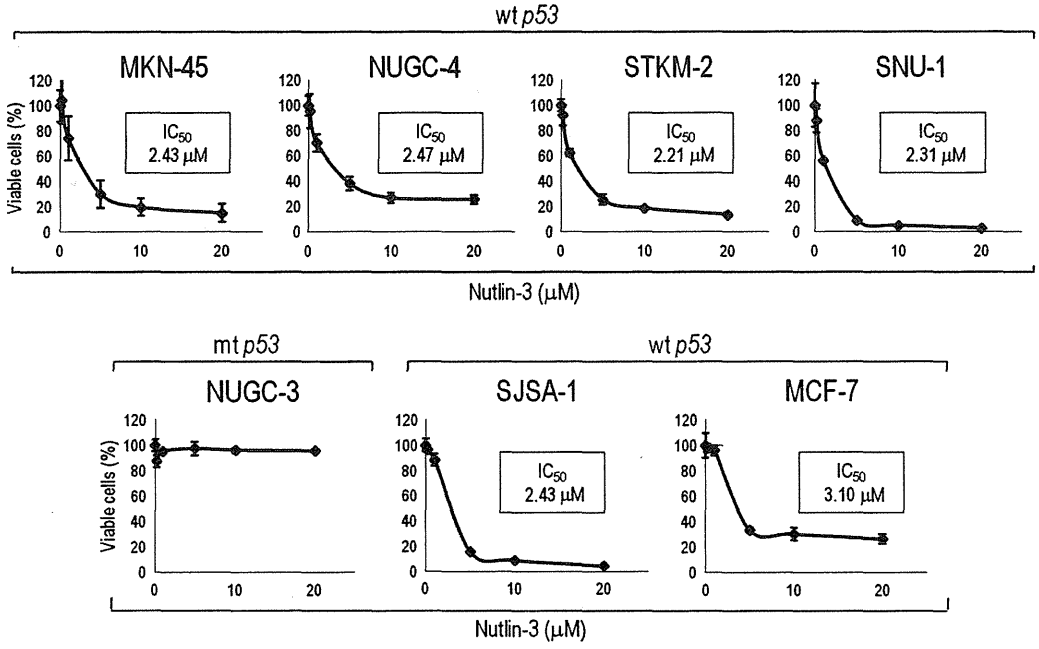

Fig. 2. Nutlin-3 inhibits the growth of gastric cancer cells with wild-type (wt) *p53*. All experiments were carried out in triplicate and the results are expressed as the mean ± SE. mt, mutant-type.

where qT is the ratio of the target gene *versus* the reference gene DNA quantity in the cell line; qN is the ratio of the target gene *versus* the reference gene DNA quantity in fibroblasts; $V^{T}_{\text{target gene}}$ is the relative DNA quantity of the target gene in the cell line; $V^{N}_{\text{target gene}}$ is the relative DNA quantity of the target in fibroblasts; $V^{T}_{\text{reference gene}}$ is the relative DNA quantity of the reference gene in the cell line; and $V^{N}_{\text{reference gene}}$ is the relative DNA quantity of the reference gene in fibroblasts.

Cell viability assays. WST-8 colorimetric assays were carried out using a Cell Counting kit-8 (Dojin Laboratories, Kumamoto, Japan) according to the manufacturer's protocol. Cells were seeded into 96-well plates at 5×10^3 cells/well with 100 μL culture medium for 24 h, treated with nutlin-3 and 5-FU for 72 h, then analyzed with an iMark microplate reader (Bio-Rad, Hercules, CA, USA).

Analysis of cell cycle and apoptosis. Cells were seeded into 60-mm dishes at 5×10^5/dish. After incubation with nutlin-3 (10 μM) or an equivalent amount of DMSO for 24 h, cells were gently lifted with Accutase (US Biotechnologies, Parker Ford, PA, USA) at room temperature for 10 min. The cells were then washed once with PBS and stained with a Cycletest Plus DNA reagent kit (BD Biosciences, Franklin Lakes, NJ, USA) according to the manufacturer's protocol. Apoptotic cells were detected by double staining with propidium iodide (PI) and annexin V labeled with FITC using an Annexin V–FITC Apoptosis Detection kit (Beckman Coulter, Brea, CA, USA) according to the manufacturer's protocol. Flow cytometry was carried out using a FACSCalibur flow cytometer and CellQuest software (both BD Biosciences). The percentage of cells in different cell cycle phases was calculated using ModFit LT (Verity Software House, Topsham, ME, USA).

Combination index. To determine whether nutlin-3 can enhance the antitumor effects of conventional chemotherapeutic agents, we used combination index (CI) and an isobologram calculated using CalcuSyn software (Cambridge, UK) according to the Chou and Talalay median effect principle.[31] In this analysis: CI > 1.3 indicates antagonism; CI = 1.1–1.3 moderate antagonism; CI = 0.9–1.1 additive effect; CI = 0.8–0.9 slight synergism; CI = 0.6–0.8 moderate synergism; CI = 0.4–0.6 synergism; and CI = 0.2–0.4 strong synergism.

***In vivo* antitumor effects of nutlin-3 and 5-FU.** Female BALB/c nude mice (5–6 weeks old) were obtained from Charles River Japan (Kanagawa, Japan) and maintained under specific pathogen-free conditions in a temperature and humidity controlled environment. MKN-45 cells were suspended in Hank's balanced salt solution (Sigma-Aldrich), and the cell concentration was adjusted to 5×10^4/μL. Then 100 μL of the adjusted cell suspension of MKN-45 was injected s.c. into the right flank of mice under anesthesia. Ten days later, the s.c. xenografted tumors grew to approximately 5–6 mm in diameter. The mice were randomly assigned to four groups ($n = 6$ per group) as follows: nutlin-3 alone (40 mg/kg), 5-FU alone (40 mg/kg), nutlin-3 (40 mg/kg) plus 5-FU (40 mg/kg), and control (DMSO). Nutlin-3, 5-FU, and DMSO were injected i.p. every 2 days for 2 weeks (six doses). Tumor volume was measured with a caliper twice a week and calculated using $V = \text{length} \times \text{width}^2 \times 0.52$, derived from the formula[32] for the volume of an ellipsoid. To monitor health, the mice were weighed every 2 days and their general physical status was recorded daily.

Statistical analysis. Statistical significance of differences between various groups was evaluated using Dunnett's or Tukey's test. A difference between the experimental groups was considered statistically significant when the P-value was <0.05.

Results

Expression of p53 and molecules regulating p53. MKN-45 cells expressed a high level of MDM2, which was slightly lower than that in SJSA-1 cells (MDM2 positive control). Enhanced MDM4 expression was detected in SNU-1 cells and the MDM4 expression level was intermediate between those in Weri-1 and MCF-7 cells (MDM4 positive controls). The other two cell lines with wt *p53* and three cell lines with mt *p53* did not express

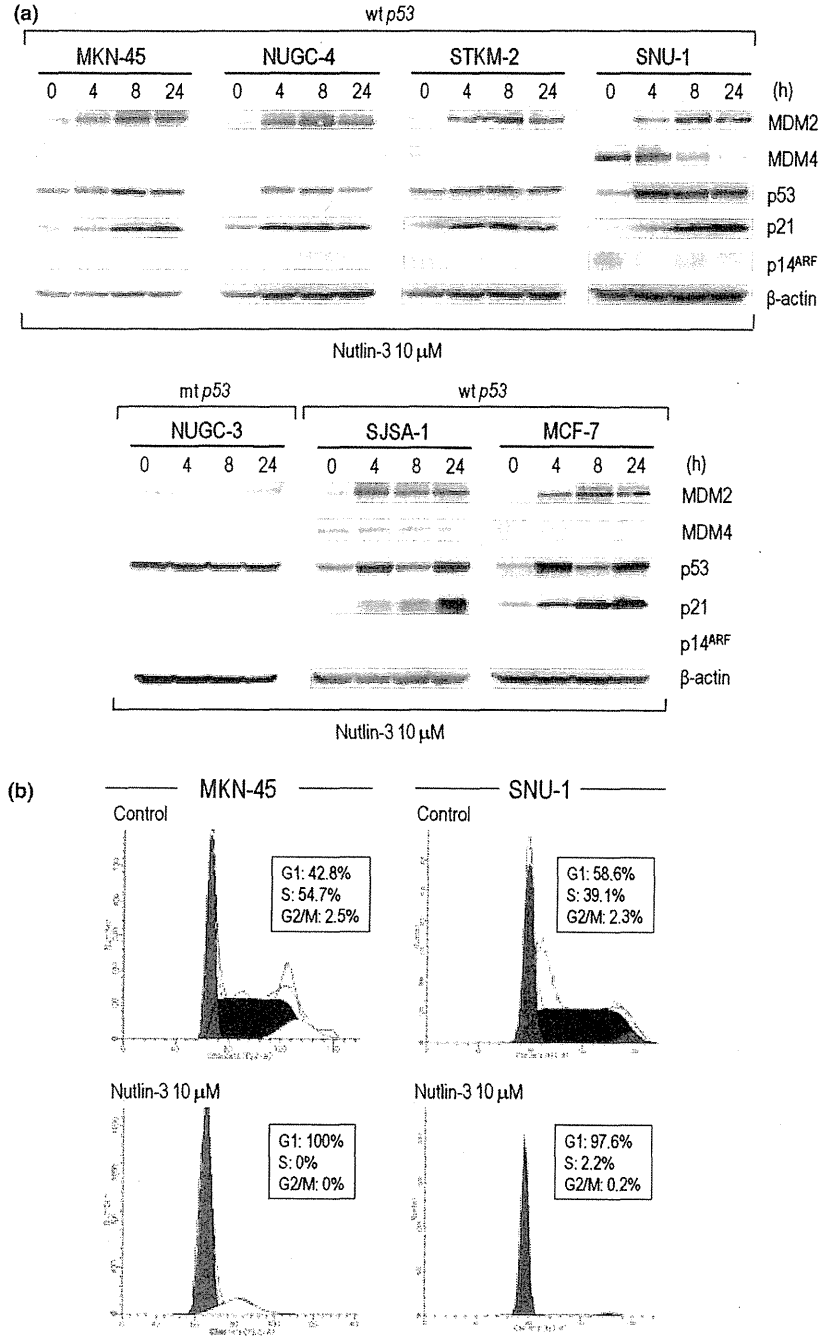

Fig. 3. Effects of nutlin-3 on p53 and $p21^{WAF1}$ expression and cell cycle distribution in gastric cancer cells with wild-type (wt) *p53*. (a) Time-course analysis of the expression of p53 and its downstream molecule $p21^{WAF1}$ in gastric cancer cells treated with nutlin-3. (b) Cell cycle distribution in gastric cancer cell lines with wt *p53* treated with nutlin-3. MDM, human homolog of murine double minute; mt, mutant-type.

either MDM2 or MDM4 at high levels (Fig. 1a). Among the wt *p53* cell lines, SJSA-1, Weri-1, MKN-45, and SNU-1 cells expressed relatively high p53 levels, whereas MCF-7, NUGC-4, and STKM-2 cells expressed lower p53 levels, indicating that the p53 level was positively related to either the MDM2 level or MDM4 level. The cell lines with mt *p53* showed very high p53 levels. $p14^{ARF}$ was detected only in STKM-1. To estimate whether p53 function is intact, four cell lines with wt *p53* (MKN-45, NUGC-4, STKM-2, and SNU-1) and one cell line with mt *p53* (NUGC-3) were exposed to various concentrations of 5-FU for 24 h then analyzed for p53 and $p21^{WAF1}$ levels. All cell lines with wt *p53* accumulated p53 and $p21^{WAF1}$, whereas the cell line with mt *p53* expressed a similar p53 level and undetectable $p21^{WAF1}$ level (Fig. 1b).

Real-time quantitative PCR analysis of *MDM2* and *MDM4* copy numbers in gastric cancer cell lines. Among the cell lines, only MKN-45 cells contained a twofold or higher *MDM2* copy number than fibroblasts. The copy number of *MDM4* in SNU-1 cells was the same as those in fibroblasts and other cell lines with wt *p53*, indicating that MDM4 protein overexpression in SNU-1 cells was not caused by gene amplification (Fig. 1c).

Effects of nutlin-3 on cell growth of gastric cancer cell lines. Gastric cancer cell lines with wt *p53* were cultured in the presence of nutlin-3 (0.2, 1, 5, 10, and 20 μM) for 3 days. A dose-dependent growth suppression was observed in all cell lines with wt *p53*. Their IC_{50} values ranged from 2.21 to 2.47 μM, which were equivalent to those of the MCF-7 and SJSA-1 cell lines (Fig. 2). Nutlin-3 most effectively decreased

doi: 10.1111/j.1349-7006.2010.01821.x

SNU-1 cell viability (94.8% at 10 μM) compared with the viability of the other cell lines (72.8–81.1%). NUGC-3 cells carrying mt *p53* were resistant to nutlin-3 (IC_{50} = 35.1 μM, data not shown).

Effects of nutlin-3 on expression of p53, MDM2, $p21^{WAF1}$, and MDM4. Both wt *p53* and mt *p53* cells were exposed to nutlin-3 (10 μM) for 0, 4, 8, and 24 h (Fig. 3). Nutlin-3 accumulated p53 as early as 4 h following exposure, with concomitant induction of MDM2 and $p21^{WAF1}$. In SNU-1 cells expressing a high MDM4 level, nutlin-3 inversely decreased MDM4 level. MDM4 expression was hardly detected in the other cell lines with wt *p53*, and nutlin-3 showed no apparent effect on its expression in these cell lines. In the NUGC-3 cell line carrying mt *p53*, nutlin-3 treatment did not increase the MDM2 expression level.

Effects of nutlin-3 on cell cycle in gastric cancer cell lines with wt *p53*. MKN-45 and SNU-1 cell lines were used for examination of cell cycle distribution after incubation with nutlin-3 (10 μM; Fig. 3b). Twenty-four hours after treatment with nutlin-3, the cell fraction of S phase decreased from 54.7% to 0% and the cell fraction of G_1 phase reciprocally increased from 42.8% to 100% in the MKN-45 cell line. Similarly, nutlin-3 exposure decreased the cell fraction of S phase from 39.1% to 2.2% and increased the cell fraction of G_1 phase from 58.6% to 97.6% in the SNU-1 cell line. These results showed that nutlin-3 induced G_1 arrest in these cell lines.

Activation of p53 by nutlin-3 and apoptotic cell death in gastric cancer cells with wt *p53*. MKN-45, NUGC-4, SUN-1, and NUGC-3 cells were exposed to nutlin-3 (10 μM) or an equivalent amount of control vehicle (DMSO) for 72 h, then tumor cells were stained with FITC–annexin V and PI. The cells were analyzed by flow cytometry; cells negative for both annexin V and PI were considered to be non-apoptotic, cells positive for annexin V only were considered to be early apoptotic, and cells positive for both annexin V and PI were considered to be late apoptotic or necrotic. Exposure of MKN-45 cells to nutlin-3 increased the fractions of the early and late phases of apoptosis from 4.6% to 28.4% and from 4.3% to 10.3%, respectively (Fig. 4a). Similar increases in populations of the early and late phases of apoptosis were observed in the other two wt *p53* cell lines (NUGC-4, SNU-1). In contrast, nutlin-3 showed no effects on the population of apoptotic NUGC-3 cells.

Next, the expressions of Noxa, a p53-responsive pro-apoptotic gene product, and cleaved PARP, a marker of caspase 3 activation, were examined in the cell lines with wt *p53* 0, 4, 8, and 24 h after exposure to nutlin-3 (10 μM). The p53 accumulation was detected as early as 4 h after nutlin-3 exposure, and this

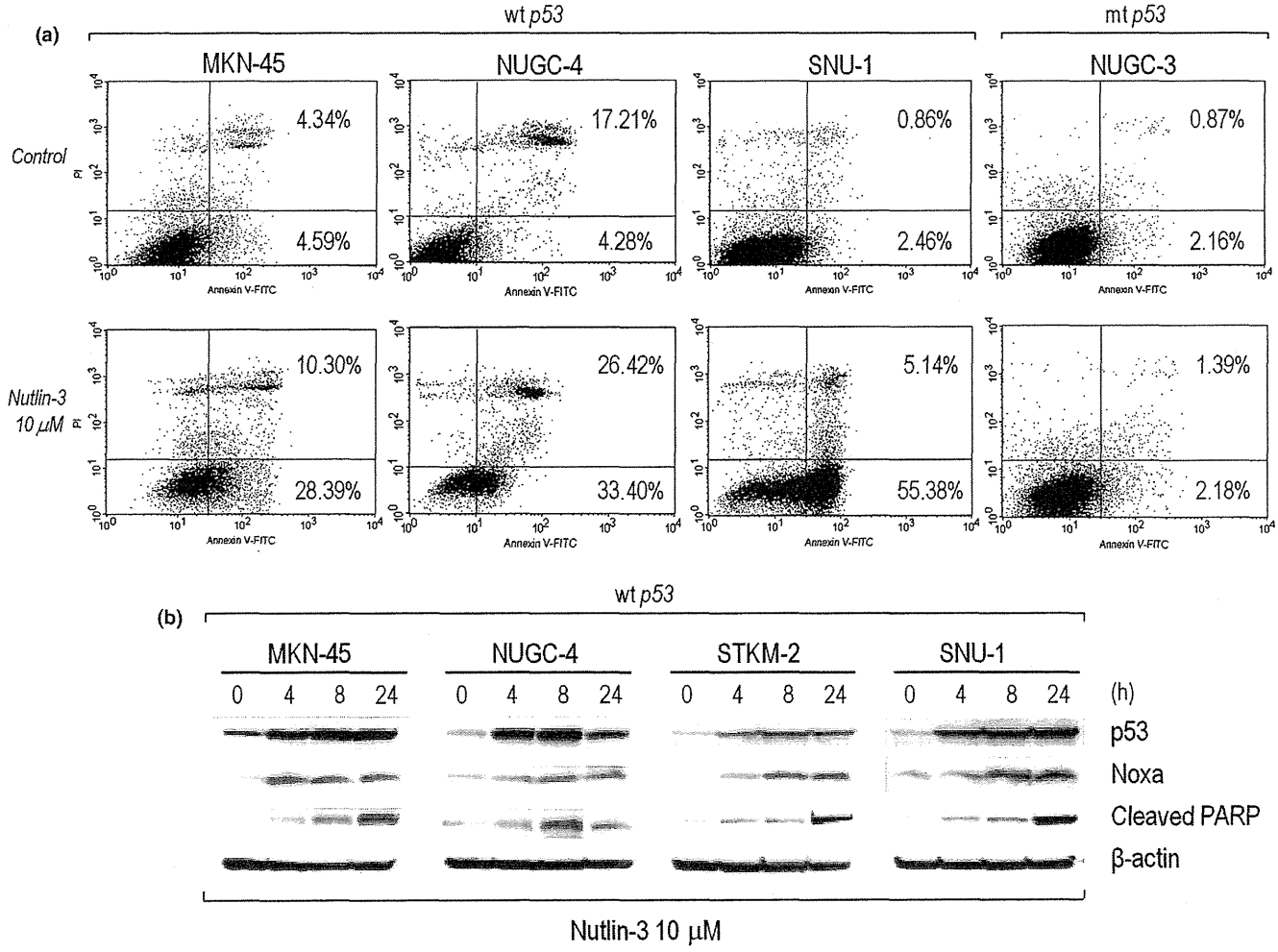

Fig. 4. Induction of apoptotic cell death by nutlin-3 in gastric cancer cell lines with wild-type (wt) *p53*. (a) Detection of apoptotic cell death in gastric cancer cell lines with wt *p53* exposed to nutlin-3. Three cell lines with wt *p53* (MKN-45, NUGC-4, and SNU-1) and one with mutant-type (mt) *p53* (NUGC-3) were treated with nutlin-3 (10 μM) or a vehicle control for 72 h. (b) Effects of nutlin-3 on expression of apoptosis-related proteins (Noxa and cleaved poly (ADP)-ribose polymerase [PARP]) in gastric cancer cell lines with wt *p53*.

accumulation was accompanied by the expression of Noxa and cleaved PARP in all four cell lines (Fig. 4b).

***In vitro* antitumor effects of 5-FU and CDDP alone or in combination with nutlin-3 in gastric cancer cells with wt *p53*.** We examined whether nutlin-3 can enhance the antitumor effects of conventional chemotherapeutic agents, 5-FU and CDDP, in gastric cancer cell lines with wt *p53*. Specifically, the cell lines with wt *p53* (MKN-45, NUGC-4, STKM-2, and SNU-1) were treated with 0.25 or 1 μM 5-FU alone or 1 μM CDDP alone or in combination with various concentrations (1, 2, and 5 μM) of nutlin-3 (Fig. 5).

The 5-FU and nutlin-3 combination showed an apparent additive effect in MKN-45, STKM-2, and SNU-1 cells but not in NUGC-4 cells. The CDDP and nutlin-3 combination showed an apparent synergistic effect in MKN-45, STKM-2, and SNU-1 cells (Table 2). NUGC-4 cells required a higher concentration of CDDP (5 μM) to achieve a synergistic effect with nutlin-3 than the other three cell lines.

***In vivo* antitumor effects of nutlin-3 alone or in combination with 5-FU.** The *in vivo* antitumor effects of nutlin-3 alone or in combination with 5-FU were analyzed in an MKN-45 xenograft tumor model in nude mice. Injections of nutlin-3 (40 mg/kg, i.p.) or 5-FU (40 mg/kg, i.p.) were well tolerated. No major adverse effects on body weight were observed in the groups of nutlin-3 alone, 5-FU alone, or 5-FU plus nutlin-3 compared with the control group. Both nutlin-3 alone and 5-FU alone significantly inhibited the growth of xenograft tumors compared with the control (Fig. 6a). The combination of these agents showed more potent growth inhibitory effects than did each agent alone.

All mice were killed on day 27, and tumors were excised and weighed. The tumor weights in the nutlin-3 and 5-FU groups were reduced to 58% and 40%, respectively, of that in the control group (Fig. 6b,c). The combination treatment decreased tumor weight to approximately 21% of the control tumor weight, and the weight was significantly less than those in mice treated with nutlin-3 alone or 5-FU alone (Fig. 6b).

Discussion

Mutation or deletion of p53 has been found in approximately 30% of gastric cancers and in approximately 50% of all cancers. This initially suggests that an impaired p53 signal is one of the abnormalities leading to carcinogenesis, and that such impairment might be less important in gastric carcinogenesis. However, abnormalities in genes regulating p53, such as $p14^{ARF}$, *MDM2*, and *MDM4*, as well as abnormalities in downstream genes regulated by p53, have been frequently observed in many

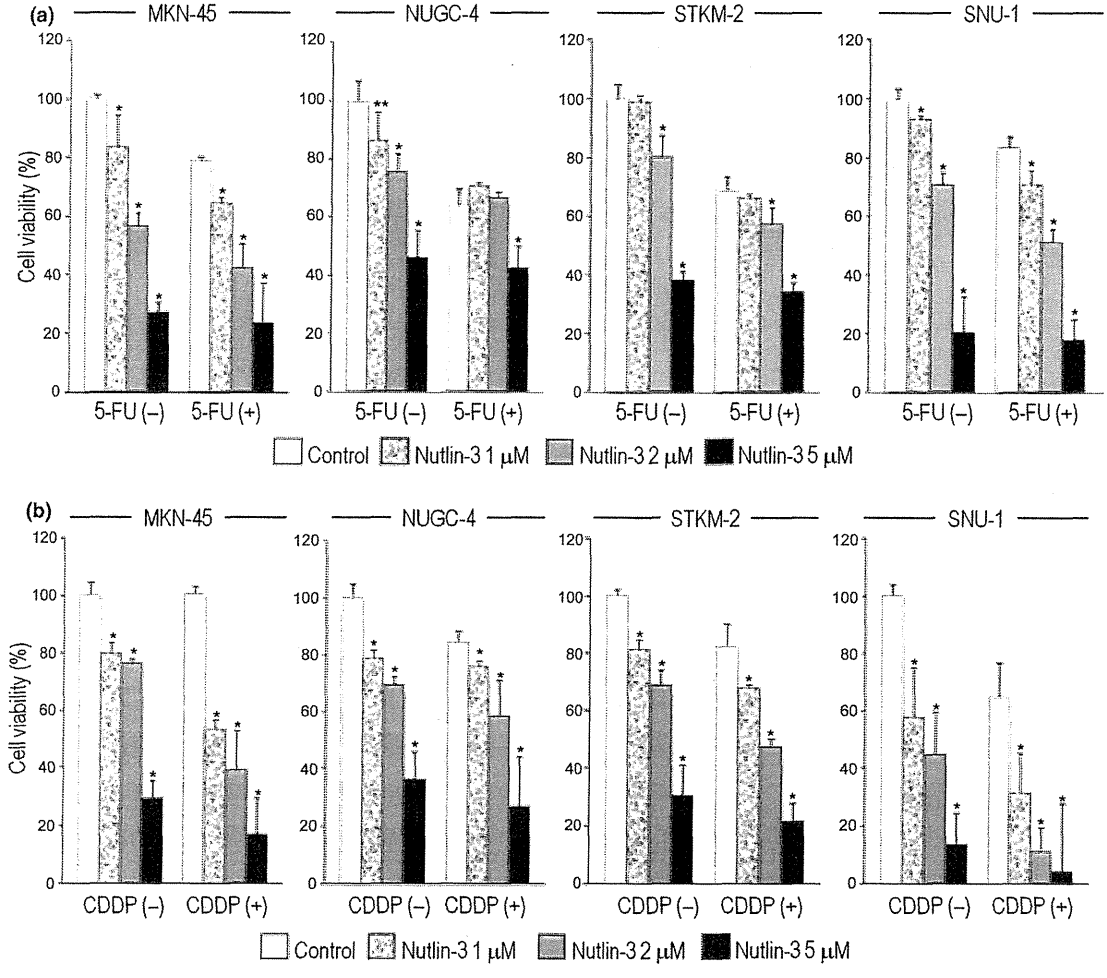

Fig. 5. Cytotoxic effects of chemotherapeutic drugs 5-fluorouracil (5-FU) and cisplatin (CDDP) and enhancement of effects by nutlin-3 in gastric cancer cells with wild-type (wt) *p53*. The cells were cultured for 72 h with the indicated concentrations of nutlin-3 and chemotherapeutic drugs. (a) 5-FU (0.25 or 1 μM) was given in combination with nutlin-3. (b) CDDP (1 μM) was given in combination with nutlin-3. Statistical significance of differences between groups was evaluated using Dunnett's test. $^{*}P < 0.01$; $^{**}P < 0.05$.

doi: 10.1111/j.1349-7006.2010.01821.x

Table 2. Combination index (CI) of nutlin-3 plus 5-fluorouracil (5-FU) or cisplatin (CDDP) for gastric cancer cells

Nutlin-3 (μM)	5-FU (μM)	CI			
		MKN-45	NUGC-4	STKM-2	SNU-1
1.00	0.25† or 1.00	1.09	2.21	1.46	1.12
2.00	0.25† or 1.00	0.90	1.56	1.20	1.02
5.00	0.25† or 1.00	0.79	1.49	0.95	0.94
	CDDP (μM)				
1.00	1.00	0.52	1.40	0.83	0.81
2.00	1.00	0.60	0.96	0.62	0.44
5.00	1.00	0.58	0.51	0.53	0.36

†MKN-45 and NUGC-4 cells were treated with 0.25 μM 5-FU. The combined cytotoxic effect of 5-FU or CDDP with nutlin-3 was determined by CI and isobologram. CI > 1.3, antagonism; CI = 1.1–1.3, moderate antagonism; CI = 0.9–1.1, additive effect; CI = 0.8–0.9, slight synergism; CI = 0.6–0.8, moderate synergism; CI = 0.4–0.6, synergism; CI = 0.2–0.4, strong synergism.

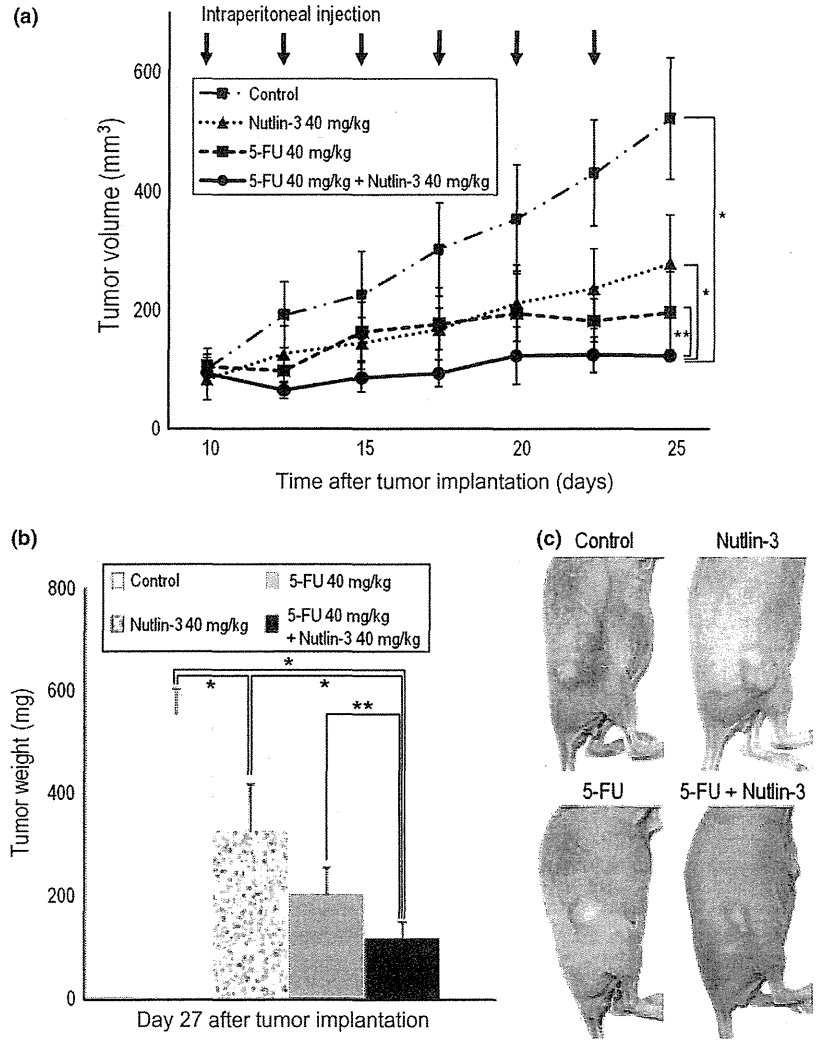

Fig. 6. *In vivo* antitumor activity of nutlin-3 in a xenograft model of a gastric cancer cell line (MKN-45) with wild-type (wt) *p53* and amplified human homolog of murine double minute 2 (*MDM2*). (a) Suppression of *in vivo* growth of MKN-45 cells by nutlin-3, 5-fluorouracil (5-FU), and nutlin-3 plus 5-FU in combination. The results are expressed as the mean ± SE. Statistical significance of differences between groups was evaluated using Dunnett's test. $*P < 0.01$; $**P < 0.05$. (b) Effects of nutlin-3 alone, 5-FU alone, and in combination, on tumor weight. Data are expressed as the mean ± SE. Statistical significance of differences between groups was evaluated using Tukey's test. $*P < 0.01$; $**P < 0.05$. (c) Representative photographs of MKN-45 tumor-bearing BALB/c nude mice treated with either vehicle control or nutlin-3 and 5-FU.

cancer cells. This led to the hypothesis that abnormality in the p53 signal pathway, which is found in almost all cancer cells, is the hallmark of cancers.[33,34] Our results indicating the efficacy of nutlin-3 in all gastric cancer cell lines with wt *p53* (Figs 2–4) are in agreement with those of recent studies investigating nutlin-3 efficacy in other malignancies.[22–24,35,36] Taken together, these results clearly support the above hypothesis that an impaired p53 signal pathway by downregulated p53 plays a critical role in the carcinogenesis of cells with wt *p53*, and the restoration of this p53 signal by nutlin-3 is indeed a very attractive therapeutic strategy for the control of cancers with wt *p53*.

SNU-1 cells with MDM4 overexpression were highly sensitive to treatment with nutlin-3 in our study. Previous studies have shown that other types of cancer cells with overexpression of MDM4 are resistant to nutlin-3.[37–39] The underlying reason for this discrepancy remains unclear. Another study has

substantiated that MDM4 reduction was caused by MDM2 accumulation as induced by nutlin-3-reactivated p53 in cancer cells overexpressing MDM4.[40] It suggests that this effect was mediated by ubiquitin ligase activity of MDM2. We showed that MDM4 in SUN-1 cells was decreased by the nutlin-3 exposure as the report pointed out, and also confirmed that the proteasome inhibitor MG132 inhibits this MDM4 reduction induced by nutlin-3 (data not shown). Therefore, MDM2 accumulation after nutlin-3 treatment was considered to facilitate MDM4 degradation in SNU-1 cells, and this might result in the susceptibility to nutlin-3 in SNU-1 cells. Another previous report suggested that the K-*Ras* oncogene and insulin-like growth factor 1 induce MDM4 expression through activation of mRNA transcription.[16] These other activation mechanisms of MDM4 might have caused the different sensitivity of MDM4 overexpressed cells to nutlin-3.

Nutlin-3 could not accumulate MDM2 in NUGC-3 cells with mt *p53* even at the high dosage of 40 μM (data not shown). We observed less expression of MDM2 in cells with mt *p53* before the exposure of nutlin-3. This indicates the disruption of normal p53–MDM2 interaction (positive feedback of accumulated p53 to MDM2), and therefore, MDM2 would not increase after nutlin-3 in NUGC-3 cells.

We found that nutlin-3 worked additively with 5-FU and synergistically with CDDP in the gastric cancer cell lines with wt *p53* (Table 2). 5-Fluorouracil and CDDP were selected as combination drugs for nutlin-3 because they are widely used for the treatment of patients with advanced gastric cancers.[41] 5-Fluorouracil is an antimetabolite that inhibits DNA and RNA synthesis, resulting in cell growth inhibition. It was previously reported that 5-FU exerts cytotoxic effects through ribosomal stress, which leads to inhibition of rRNA processing and inhibition of MDM2–p53 interaction.[42–45] This mechanism of p53 activation by 5-FU might be similar to that by nutlin-3, therefore these two drugs might occasionally work competitively, providing a possible explanation as to why the antitumor effect of 5-FU was not always enhanced synergistically by nutlin-3. In contrast, CDDP inhibits DNA function directly by DNA intercalation, resulting in DNA damage and p53 activation.[46] It has recently been reported that nutlin-3 does not diminish CDDP-induced p53 activation.[47] Moreover, proapoptotic responses, including caspase 3 and caspase 7, have been shown to be significantly enhanced with the nutlin-3 and CDDP combination in cancer cells with wt *p53*.[36]

Nutlin-3 induced p53 accumulation, and 5-FU, which is a key drug in clinical chemotherapy for advanced gastric cancer, exerted an additive antitumor effect against MKN-45 *in vitro*. Moreover, no reports have been published indicating the antitumor effects of combined treatment with 5-FU and nutlin-3 in animal experiments. Therefore, we carried out *in vivo* experiments using a xenograft tumor model of the MDM2 overexpressed cell line MKN-45 and found that the antitumor effects of 5-FU plus nutlin-3 were superior to those of either agent alone without major adverse effects, including body weight loss and diarrhea (Fig. 6).

In conclusion, nutlin-3 alone or in combination with conventional anticancer agents is a novel therapeutic strategy for gastric cancer with wt *p53*.

Acknowledgments

This work was supported in part by Grants-in-Aid from the Ministry of Education, Culture, Sports, Science and Technology of Japan (to I.H.), the Japan Society for the Promotion of Science (to K.Y.), and the Ministry of Health Labor and Welfare of Japan (to K.Y.).

Disclosure Statement

The authors have no conflict of interest.

References

1 Teodoro JG, Evans SK, Green MR. Inhibition of tumor angiogenesis by p53: a new role for the guardian of the genome. *J Mol Med* 2007; **85**: 1175–86.
2 Fridman JS, Lowe SW. Control of apoptosis by p53. *Oncogene* 2003; **22**: 9030–40.
3 Vousden KH, Lu X. Live or let die: the cell's response to p53. *Nat Rev Cancer* 2002; **2**: 594–604.
4 Feki A, Irminger-Finger I. Mutational spectrum of p53 mutations in primary breast and ovarian tumors. *Crit Rev Oncol Hematol* 2004; **52**: 103–16.
5 Hjortsberg T, Rubio-Nevado JM, Hamroun D, Claustre M, Béroud C, Soussi T. *The p53 Mutation HandBook v 2.* 2008. [Cited 29 Nov 2010.] Available from URL: http://p53.free.fr/Database/p53_mutation_HB.html
6 Soussi T, Asselain B, Hamroun D *et al.* Meta-analysis of the p53 mutation database for mutant p53 biological activity reveals a methodologic bias in mutation detection. *Clin Cancer Res* 2006; **12**: 62–9.
7 Toledo F, Wahl GM. MDM2 and MDM4: p53 regulators as targets in anticancer therapy. *Int J Biochem Cell Biol* 2007; **39**: 1476–82.
8 Michael D, Oren M. The p53-Mdm2 module and the ubiquitin system. *Semin Cancer Biol* 2003; **13**: 49–58.
9 Momand J, Jung D, Wilczynski S, Niland J. The MDM2 gene amplification database. *Nucleic Acids Res* 1998; **26**: 3453–9.
10 Schuler M, Green DR. Transcription, apoptosis and p53: catch-22. *Trends Genet* 2005; **21**: 182–7.
11 Schuler M, Maurer U, Goldstein JC *et al.* p53 triggers apoptosis in oncogene-expressing fibroblasts by the induction of Noxa and mitochondrial Bax translocation. *Cell Death Differ* 2003; **10**: 451–60.
12 Oliner JD, Kinzler KW, Meltzer PS, George DL, Vogelstein B. Amplification of a gene encoding a p53-associated protein in human sarcomas. *Nature* 1992; **358**: 80–3.
13 Gunther T, Schneider-Stock R, Hackel C *et al.* Mdm2 gene amplification in gastric cancer correlation with expression of Mdm2 protein and p53 alterations. *Mod Pathol* 2000; **13**: 621–6.
14 Sun LP, Jiang NJ, Fu W, Xue YX, Zhao YS. Relationship between gastric cancer and gene amplification of p14 and mdm2. *Ai Zheng* 2004; **23**: 36–9.
15 Marine JC, Dyer MA, Jochemsen AG. MDMX: from bench to bedside. *J Cell Sci* 2007; **120**: 371–8.
16 Gilkes DM, Pan Y, Coppola D, Yeatman T, Reuther GW, Chen J. Regulation of MDMX expression by mitogenic signaling. *Mol Cell Biol* 2008; **28**: 1999–2010.
17 Laurie NA, Donovan SL, Shih CS *et al.* Inactivation of the p53 pathway in retinoblastoma. *Nature* 2006; **444**: 61–6.
18 Stad R, Ramos YF, Little N *et al.* Hdmx stabilizes Mdm2 and p53. *J Biol Chem* 2000; **275**: 28039–44.
19 Stad R, Little NA, Xirodimas DP *et al.* Mdmx stabilizes p53 and Mdm2 via two distinct mechanisms. *EMBO Rep* 2001; **2**: 1029–34.
20 Vassilev LT, Vu BT, Graves B *et al.* In vivo activation of the p53 pathway by small-molecule antagonists of MDM2. *Science* 2004; **303**: 844–8.
21 Vassilev LT. MDM2 inhibitors for cancer therapy. *Trends Mol Med* 2007; **13**: 23–31.
22 Logan IR, McNeill HV, Cook S, Lu X, Lunec J, Robson CN. Analysis of the MDM2 antagonist nutlin-3 in human prostate cancer cells. *Prostate* 2007; **67**: 900–6.
23 Van Maerken T, Speleman F, Vermeulen J *et al.* Small-molecule MDM2 antagonists as a new therapy concept for neuroblastoma. *Cancer Res* 2006; **66**: 9646–55.
24 Drakos E, Thomaides A, Medeiros LJ *et al.* Inhibition of p53-murine double minute 2 interaction by nutlin-3A stabilizes p53 and induces cell cycle arrest and apoptosis in Hodgkin lymphoma. *Clin Cancer Res* 2007; **13**: 3380–7.
25 Yokozaki H. Molecular characteristics of eight gastric cancer cell lines established in Japan. *Pathol Int* 2000; **50**: 767–77.
26 Iida S, Akiyama Y, Nakajima T *et al.* Alterations and hypermethylation of the p14(ARF) gene in gastric cancer. *Int J Cancer* 2000; **87**: 654–8.
27 Kim SY, Kim JE, Lee KW, Lee HJ. *Lactococcus lactis* ssp. lactis inhibits the proliferation of SNU-1 human stomach cancer cells through induction of G0/G1 cell cycle arrest and apoptosis via p53 and p21 expression. *Ann N Y Acad Sci* 2009; **1171**: 270–5.
28 Yamato K, Yamada T, Kizaki M *et al.* New highly potent and specific E6 and E7 siRNAs for treatment of HPV16 positive cervical cancer. *Cancer Gene Ther* 2008; **15**: 140–53.

doi: 10.1111/j.1349-7006.2010.01821.x

29 Szabo A, Perou CM, Karaca M *et al.* Statistical modeling for selecting housekeeper genes. *Genome Biol* 2004; **5**: R59.
30 Konigshoff M, Wilhelm J, Bohle RM, Pingoud A, Hahn M. HER-2/neu gene copy number quantified by real-time PCR: comparison of gene amplification, heterozygosity, and immunohistochemical status in breast cancer tissue. *Clin Chem* 2003; **49**: 219–29.
31 Chou TC, Talalay P. Quantitative analysis of dose-effect relationships: the combined effects of multiple drugs or enzyme inhibitors. *Adv Enzyme Regul* 1984; **22**: 27–55.
32 Geran R, Greenberg N, MacDonald M, Schumacher A, Abbott B. Protocols for screening chemical agents and natural products against animal tumors and other biological systems. *Cancer Chemother Rep* 1972; **3**: 1–88.
33 Vogelstein B, Lane D, Levine AJ. Surfing the p53 network. *Nature* 2000; **408**: 307–10.
34 Sherr CJ, McCormick F. The RB and p53 pathways in cancer. *Cancer Cell* 2002; **2**: 103–12.
35 Kojima K, Konopleva M, Samudio IJ *et al.* MDM2 antagonists induce p53-dependent apoptosis in AML: implications for leukemia therapy. *Blood* 2005; **106**: 3150–9.
36 Bauer S, Muhlenberg T, Leahy M *et al.* Therapeutic potential of Mdm2 inhibition in malignant germ cell tumours. *Eur Urol* 2009; **57**: 679–87.
37 Wade M, Wong ET, Tang M, Stommel JM, Wahl GM. Hdmx modulates the outcome of p53 activation in human tumor cells. *J Biol Chem* 2006; **281**: 33036–44.
38 Patton JT, Mayo LD, Singhi AD, Gudkov AV, Stark GR, Jackson MW. Levels of HdmX expression dictate the sensitivity of normal and transformed cells to Nutlin-3. *Cancer Res* 2006; **66**: 3169–76.
39 Hu B, Gilkes DM, Farooqi B, Sebti SM, Chen J. MDMX overexpression prevents p53 activation by the MDM2 inhibitor Nutlin. *J Biol Chem* 2006; **281**: 33030–5.
40 Xia M, Knezevic D, Tovar C, Huang B, Heimbrook DC, Vassilev LT. Elevated MDM2 boosts the apoptotic activity of p53-MDM2 binding inhibitors by facilitating MDMX degradation. *Cell Cycle* 2008; **7**: 1604–12.
41 Ajani JA, Rodriguez W, Bodoky G *et al.* Multicenter phase III comparison of cisplatin/S-1 with cisplatin/infusional fluorouracil in advanced gastric or gastroesophageal adenocarcinoma study: the FLAGS trial. *J Clin Oncol* 2010; **28**: 1547–53.
42 Kanamaru R, Kakuta H, Sato T, Ishioka C, Wakui A. The inhibitory effects of 5-fluorouracil on the metabolism of preribosomal and ribosomal RNA in L-1210 cells in vitro. *Cancer Chemother Pharmacol* 1986; **17**: 43–6.
43 Ghoshal K, Jacob ST. Specific inhibition of pre-ribosomal RNA processing in extracts from the lymphosarcoma cells treated with 5-fluorouracil. *Cancer Res* 1994; **54**: 632–6.
44 Bunz F, Hwang PM, Torrance C *et al.* Disruption of p53 in human cancer cells alters the responses to therapeutic agents. *J Clin Invest* 1999; **104**: 263–9.
45 Sun XX, Dai MS, Lu H. 5-fluorouracil activation of p53 involves an MDM2-ribosomal protein interaction. *J Biol Chem* 2007; **282**: 8052–9.
46 Johnson N, Butour J-L, Villani G, Wimmer F, Defais M, Pierson V. Metal antitumor compounds: the mechanism of action of platinum complexes. *Prog Clin Biochem Med* 1989; **10**: 1–24.
47 Barbieri E, Mehta P, Chen Z *et al.* MDM2 inhibition sensitizes neuroblastoma to chemotherapy-induced apoptotic cell death. *Mol Cancer Ther* 2006; **5**: 2358–65.

厚生労働科学研究費補助金

第３次対がん総合戦略研究事業

ヒトパピローマウイルスを標的とする発がん予防の研究

平成２２年度～２５年度　総合研究報告書

Ⅲ　研究成果の刊行物・別冊
その２

研究代表者　温川　恭至

平成２６（２０１４）年　５月

Ⅲ　研究成果の刊行物・別冊

その２

平成２３年度

Am J Cancer Res 2011;1(7):869-881
www.ajcr.us /ISSN:2156-6976/ajcr0000079

Original Article

An in vitro multistep carcinogenesis model for both HPV-positive and -negative human oral squamous cell carcinomas

Yusuke Zushi[1,2], Mako Narisawa-Saito[1], Kazuma Noguchi[2], Yuki Yoshimatsu[1,3], Takashi Yugawa[1], Nagayasu Egawa[1], Masatoshi Fujita[1,4], Masahiro Urade[2], Tohru Kiyono[1]

[1]Division of Virology, National Cancer Center Research Institute, 5-1-1 Tsukiji, Chuo-ku, Tokyo 104-0045, Japan; [2]Department of Oral and Maxillofacial Surgery, Hyogo College of Medicine, 1-1 Mukogawa-cho, Nishinomiya, Hyogo 663-8501, Japan; [3]Program in Cancer Biology, Fred Hutchinson Cancer Research Center, Seattle WA98109-1024, USA; [4]Department of Cellular Biochemistry, Graduate School of Pharmaceutical Sciences, Kyushu University, 3-1-1 Maidashi, Higashi-ku, Fukuoka, 812-8582, Japan.

Received July 12, 2011; accepted August 6, 2011; Epub August 18, 2011; published August 30, 2011

Abstract: Oral squamous cell carcinomas (OSCCs) are considered to arise from human oral keratinocytes. DNAs of human papillomaviruses (HPVs), predominantly types 16 and 18, etiological agents of cervical cancer, have been detected in approximately 25% of OSCCs. In accordance with the established role of E6 and E7 in inactivating p53 and pRB, respectively, mutations of p53 and inactivation of $p16^{INK4a}$ are frequently observed in HPV-negative OSCCs. In addition, other alterations such as overexpression of epidermal growth factor receptor (EGFR) are often observed in both HPV-positive and -negative OSCCs. However, causal-relationships between accumulation of these abnormalities and multi-step carcinogenesis are not fully understood. To elucidate underlying processes, we transduced either HPV16 E6/E7 or mutant CDK4 ($CDK4^{R24C}$), cyclin D1 and human telomerase reverse transcriptase (TERT) into primary human tongue keratinocytes (HTK), and obtained immortal cell populations, HTK-16E6E7 and HTK-K4DT. Additional transduction of oncogenic HRAS or EGFR together with MYC into the HTK-16E6E7 and dominant-negative p53 expressing HTK-K4DT resulted in anchorage-independent growth and subcutaneous tumor formation in nude mice. These results indicate that either HRAS mutation or activation of EGFR in cooperation with MYC overexpression play critical roles in transformation of HTKs on a background of inactivation of the pRB and p53 pathways and telomerase activation. This in vitro model system recapitulating the development of OSCCs should facilitate further studies of mechanisms of carcinogenesis in the oral cavity.

Keywords: Oral squamous cell carcinoma, HPV, carcinogenesis, human tongue keratinocytes, EGFR, HRAS, MYC

Introduction

Oral cancers are the 6th most common human neoplasms accounting for 3% of all newly diagnosed cancers[1], with about 300,000 new cases being diagnosed every year worldwide [2, 3]. Despite efforts to improve the survival rates, these have basically remained unchanged for the last 20 years. Since 50 to 70% of patients die within 5 years due to local recurrence, invasion or metastasis to the cervical lymph nodes and/or lung, or second primary cancers, generally elsewhere in the oral cavity (in line with the 'field cancerization' theory), the prognosis is poor. Moreover, oral cancers have a severe impact on the quality of life of patients and survivors. In spite of the clinical importance, we are far away from having a complete understanding of the molecular mechanisms of initiation and progression of oral cancers.

The main accepted risk factors are tobacco usage and alcohol consumption but recently, human papillomaviruses (HPV) have also been postulated to play roles [4-6]. While more than 95% of cervical squamous cell carcinomas are linked to persistent HPV infection, the presence of the HPV genome in oral cancers is reported to range from 10 to 70%, depending on the area, the ethnicity of the patients, the type of

specimen and the detection method [4]. Several studies have provided evidence that chronic infection in basal cells of the oral mucosa with high-risk HPVs, especially type 16 and 18, can promote oral carcinogenesis [7]. Two viral oncoproteins, E6 and E7, are thought to contribute to tumor progression by inactivating p53 and retinoblastoma tumor suppressor (pRB), respectively [8, 9]. E6 facilitates the degradation of p53 through its association with an accessory protein, E6-AP, a component of the ubiquitin proteolytic pathway [9]. E7 proteins of the high-risk types bind to pRB [10], leading to altered activity of this cell-cycle regulator. However, epidemiological studies and experimental data indicate that the viral presence is not enough to induce cancers even in the cervix and the requirement of additional cellular factors are especially suggested in the case of oral carcinogenesis, the roles of HPV are still under estimation.

More than 90% of oral cancers are histopathologically squamous cell carcinomas (SCCs). The development of oral squamous cell carcinomas (OSCCs) is a multistep process, starting from hyperplasia and dysplasia, and finally progressing to neoplasms (benign and malignant) [11, 12]. During these steps, multiple genetic alterations may occur, including chromosomal aberrations, DNA mutations, amplification or deletions and/or epigenetic alterations. Numerous studies have revealed that oncogenes such as EGFR, ERBB2, HRAS, KRAS, and c-MYC (MYC) are often activated by overexpression, amplification, and/or mutation [1, 13-20]. As with other carcinomas, telomerase activation is also common in oral cancers [21, 22]. In addition, mutations of p53 and disruption of the pRB pathway ($p16^{INK4a}$-CDK4/cyclin D1-pRB) are frequently observed [23-27]. Although such genetic changes have been identified, how they individually contribute to oral carcinogenesis has yet to be clarified in detail.

Recently, we have established in vitro multi-step carcinogenesis models for cervical cancer and epithelial ovarian cancer, respectively with and without HPV16 E6/E7 as transgenes [28, 29]. In the present study, taking advantage of this background, we could successfully induce tumorigenic transformation of normal human tongue keratinocytes with defined genetic elements so as to establish in vitro multistep carcinogenesis models for both HPV-positive and -negative OSCCs.

Materials and methods

Isolation of human tongue keratinocytes (HTKs)

Tongues were obtained from two tongue mucocele patients undergoing cystectomy at Hyogo College of Medicine Hospital, Japan. The Ethics Committee of Hyogo College of Medicine and National Cancer Center approved this study and the subjects gave informed consent for participation. The tongues were grossly normal and no pathological lesions were observed on subsequent histological examination. After collagenase digestion under aseptic conditions, HTK cells were obtained by scraping with a surgical blade and maintained in Epilife (Invitrogen, Carlsbad, CA).

Viral vector construction and viral transduction

Construction of the retroviral expression vectors, pCLXSN-16E6E7, pCLXSH-TERT, pCMSCVpuro-MYC, -MYC^{T58A}, pCMSCVbsd-MYC, -MYC^{T58A}, pCMSCVbsd-$HRAS^{G12V}$, pCMSCVbsd was described previously [28-30] Wild type EGFR ($EGFR^{WT}$) and a constitutive active form of EGFR ($EGFR^{d746-750}$; deletion from E746 to A750) generated by site-directed mutagenesis were similarly recombined with the retroviral vector pDEST-PQCXIP by the LR reaction (Invitrogen) to generate pQCXIP-$EGFR^{WT}$ and pQCXIP-$EGFR^{d746-750}$. The production of recombinant retroviruses was as described previously [31]. Construction of lentiviral vectors, CSII-CMV-TERT, CSII-CMV-cyclin D1, CSII-CMV-$CDK4^{R24C}$ and CSII-CMV-DNp53 and the production of recombinant lentiviruses with the vesicular stomatitis virus G glycoprotein (VSV-G) were as detailed earlier [29, 32]. Following the addition of recombinant viral fluid to cells in the presence of 4 mg/ml polybrene, infected cells were selected in the presence of 50 mg/ml of G418, 1 mg/ml of puromycin, 1 mg/ml of blasticidine-S or 50 mg/ml of hygromycin-B.

Telomerase activity

Telomerase activity was detected using a non-radioisotopic method with a TRAPeze telomerase detection kit (Intergen, Burlington, MA), as previously described [33].

Western blot analysis

Western blotting was conducted as described prviously [33]. Antibodies against cyclin D1

(clone G124-326), CDK4(clone 97), $p16^{INK4a}$ (clone G175-405; BD Biosciences, Franklin Lakes, NJ), p53 (clone DO-1; Merck, Darmstadt, Germany), $p21^{WAF1}$ (12D1; Oncogene Research Products, Cambridge, MA), MYC (sc-42), β-actin (sc-1616; Santa Cruz, CA), HPV16 E6 (clone 47A4)[34], HPV16 E7 (clone 8C9; Invitrogen) and keratin 14 (AF14; Covance, Princeton, NJ) were used as probes, and horseradish peroxidase-conjugated anti-mouse, anti-rabbit (Jackson Immunoresearch Laboratories, West Grove, PA) or anti-goat (sc-2033; Santa Cruz) immunoglobulins were employed as secondary antibodies.

Colony formation in soft agar (anchorage-independent growth)

Cells were seeded at 5×10^4 cells per 35-mm plate (BD Biosciences) in Epilife with 0.4 % agarose. Colonies over 50μm in diameter were counted after a lapse of 3 weeks. Five photographs of randomly selected areas in each dish were taken at the magnification of ×40. The numbers of colonies were measured with the COLONY program (Fujifilm, JAPAN). The experiments were performed in triplicate.

Tumorigenesis in nude mice

All surgical procedures and care administered to the animals were in accordance with institutional guidelines. Cells were resuspended in 50% Matrigel (BD Biosciences) and injected subcutaneously into a flank or orthotopically into female 6 to 7-week old BALB/c nude mice (Clea Japan Inc., Tokyo, Japan).

Immunohistochemical examination

Formalin-fixed and paraffin-embedded tissue sections (4 micrometer-thick) were deparaffinized in xylene and rehydrated through a series of graded ethanols (100–70%). For antigen retrieval, slides were immersed in a citrate buffer (pH6.4) and heated for 15 minutes in a microwave. The slides were then incubated in methanol containing 0.3% H_2O_2 to inhibit endogenous peroxidase activity. After washing, primary antibody against keratin 14 (1:500, SP53, Spring Bioscience, Pleasanton, CA) was applied for 1 h and binding was detected using an Envision Kit (Dako Cytomation; K4006). Color development was achieved with 3, 3-diaminobenzine (DAB) as chromogen and hematoxylin counterstaining. As a negative control, we used normal non-immune serum from the same source as the primary antibody.

Results

Immortalization of HTK cells with or without viral oncogenes

To establish an in vitro model system for HPV-positive OSCCs, two independent batches of primary HTK cells (HTK1 and HTK3T) were transduced with retroviral vectors expressing HPV16 E6 and E7 (HTK1-E6E7). HTK3 cells were transduced with TERT first since HPV16 E6 and E7 are not sufficient to avoid telomere erosion. Pooled populations of these HTK cells were named HTK1-E6E7 and HTK3-TE6E7, respectively. Expression of the transgenes was confirmed by immunoblotting (**Figure 1A**). As expected, decreased levels of p53 were observed in these cells (**Figure 1A**). We have shown that both telomerase activation and inactivation of the $p16^{INK4a}$/pRB pathway are required for immortalization of human primary epithelial cells. Disruption of the pRB pathway, such as inactivation of $p16^{INK4a}$ and overexpression of cyclin D1, are also frequently observed in OSCCs. In order to establish an in vitro model system for HPV16-negative OSCCs, a mutant form of CDK4 ($CDK4^{R24C}$), which cannot be inactivated by p16, and cyclin D1 as well as TERT were transduced into HTK cells (HTK1 and HTK3) with lentiviral vectors (**Figure 1B**). Pooled populations of these HTK cells were named HTK1-K4DT and HTK3-K4DT, respectively. Expression of the transgenes was confirmed by immunoblotting (**Figure 1B**) and the TRAP assay (**Figure 1C**). As expected, the combination of HPV16 E6E7 or $CDK4^{R24C}$, cyclin D1 and TERT resulted in extended life span and virtual immortalization of HTK cells (**Figure 1D**). Both the primary and immortalized cell lines expressed keratin 14, a marker of keratinocytes (data not shown). HTK1 cells showed normal diploidy and HTK1-K4DT cells was almost diploid though HTK3-K4DT cells tended to be tetraploid with some chromosomal abnormalities.

Combined transduction of HRAS and MYC into HTK1-K4DT-DNp53 and HTK1-E6E7 cells induces anchorage-independent growth and tumor-forming ability in nude mice.

In HPV-negative OSCCs, overexpression of MYC

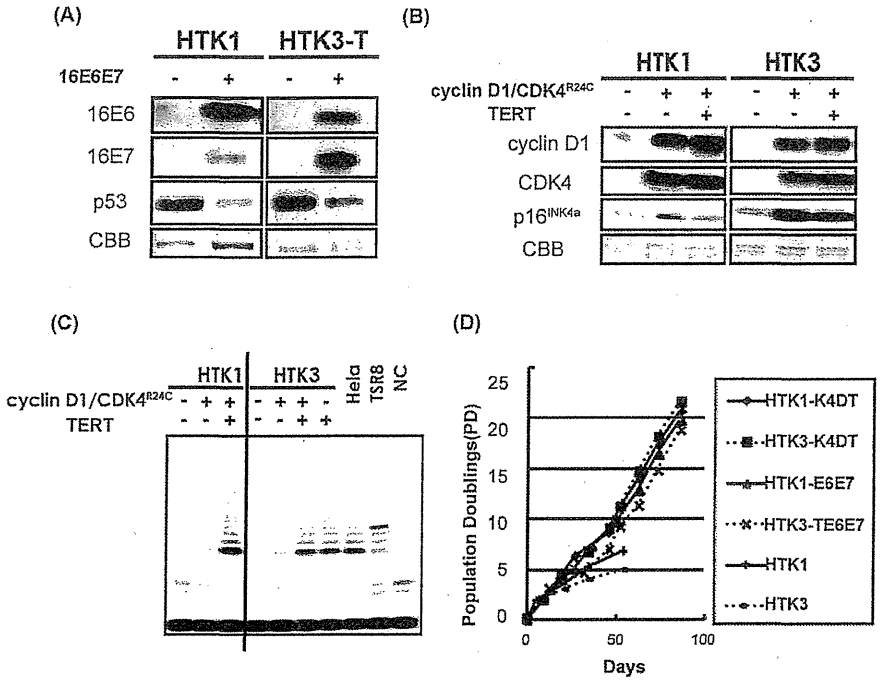

Figure 1. Immortalization of primary human tongue keratinocytes. (**A**) Two batches of primary human tongue keratinocyte (HTK), termed HTK1 and HTK3, were transduced with retroviruses expressing HPV 16 E6 and E7 for the HPV-positive OSCC model. After selection, cells were harvested and subjected to SDS-PAGE. Western blotting confirmed expression of the two transgenes in the resultant cell populations and showed endogenous expression of p53. (**B**) HTK1 and HTK3 were infected with lentiviruses expressing mutant CDK4, cyclin D1 and TERT for the HPV-negative OSCC model. Western blotting confirmed expression of the two transgenes in the resultant cell populations and showed endogenous expression of $p16^{INK4a}$. (**C**) Telomerase activity of primary and immortalized HTK cells was measured by the TRAP assay. Hela cells, eight tandem repeats of the telomeric sequence (TSR8) and CHAPS buffer alone (NC) were used as controls. (**D**) Growth curves of HTK1 and HTK3 cell lines. Day 0 is the time when the immortalizing genes (mutant CDK4, cyclin D1 and TERT) or HPV 16 E6E7 were transduced.

and mutation of HRAS and p53 are frequently observed especially in tobacco *chewing individuals for HRAS [35]*. Thus, a dominant negative form of p53 (DNp53), $HRAS^{G12V}$ and MYC were serially transduced into HTK1-K4DT cells. Expression of these transgenes together with accumulation of p53 and downregulation of $p21^{WAF1}$ was confirmed by immunoblotting (**Figure 2A**). Then we assessed the effects of oncogenic $HRAS^{G12V}$ and MYC on cell growth. HTK1-K4DT-DNp53 cells with $HRAS^{G12V}$ and MYC grew faster than those with an empty vector (**Figure 2B**), and formed numerous and much larger colonies in soft agar medium than those with $HRAS^{G12V}$ alone, whereas cells with empty vector formed no colonies (**Figure 2C**). HTK1-K4DT-DNp53 cells with $HRAS^{G12V}$ and MYC or a mutant form of MYC (MYC^{T58A}), which is resistant to proteosomal degradation, formed tumors in nude mice, whereas those without MYC failed to form tumors (**Table 1**). HTK1-K4DT-$HRAS^{G12V}$-MYC cells, which did not express a dominant negative form of p53 developed tumors less efficiently and with a long latent period, while HTK1-K4DT-DNp53 cells with MYC alone did not form tumors (**Table 1**).

For the HPV-positive OSCC model, we transduced $HRAS^{G12V}$ and MYC serially into HTK1-E6E7 cells and confirmed expression of transgenes by immunoblotting (**Figure 2D**). HTK1-E6E7 cells expressing $HRAS^{G12V}$ and MYC or $HRAS^{G12V}$ alone grew faster than those with empty vectors (**Figure 2E**). HTK1-E6E7 cells expressing $HRAS^{G12V}$ and MYC formed numerous large colonies and those expressing $HRAS^{G12V}$ alone formed some small colonies, whereas those with empty vectors formed no colonies

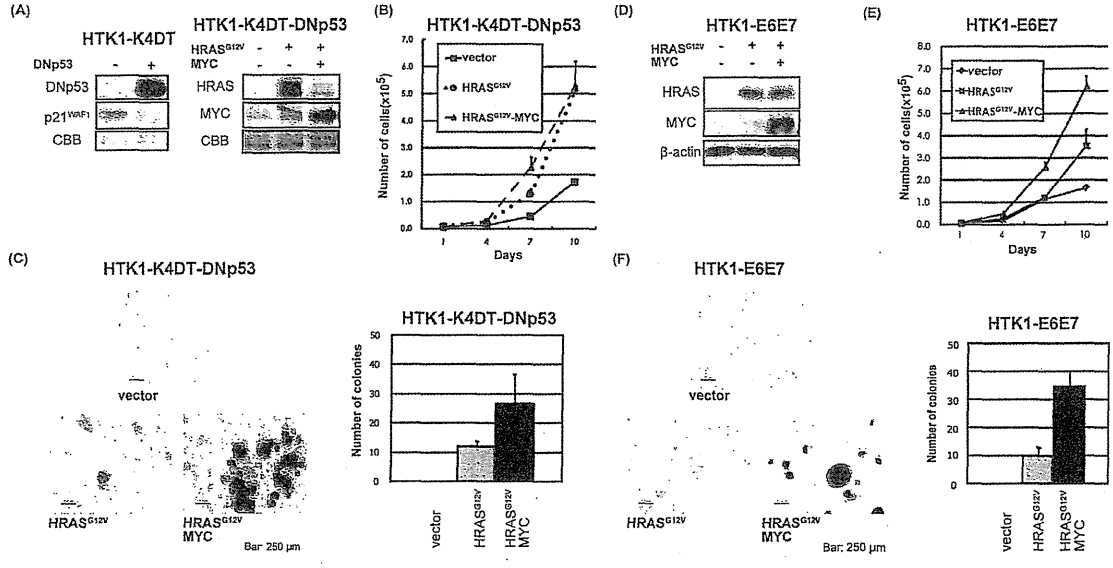

Figure 2. Anchorage-dependent and -independent growth of HTK1-E6E7-HRAS^{G12V}-MYC and HTK1-K4DT-DNp53-HRAS^{G12V}-MYC cells. (**A**) HTK1-K4DT cells were serially infected with lentiviruses encoding DNp53 and retroviruses encoding HRAS^{G12V}, MYC or empty vectors (-). After selection, cells were harvested and subjected to SDS-PAGE. Western blots show expression of the three transgenes and suppression of p21^{WAF1}. (**B**) Growth curves for DNp53-vector, DNp53-HRAS^{G12V} or DNp53-HRAS^{G12V}-MYC expressing HTK1-K4DT cells. HTK1-K4DT-DNp53-HRAS^{G12V} cells showed the fastest growth rate. Cells (2×10^4) were cultured in triplicate 12-well plates and counted every 3 days. The graphs illustrate means + s.d. (**C**) Anchorage independent growth of HTK1-K4DT cells expressing different transgenes. Cells (5×10^4) were seeded in 35-mm plates. After 3 weeks, colonies was counted when sized > 50 μm in diameter. The experiments were performed in triplicate and the total number of colonies in a 15 mm^2 area was counted. The graphs illustrate means + s.d. Scale bars, 250 μm. (**D**) HTK1-E6E7 cells were serially infected with retroviruses encoding HRAS^{G12V}, MYC or empty vectors (-). After selection, cells were harvested and subjected to SDS-PAGE. Western blots show expression of the two transgenes. (**E**) Growth curves for vector, HRAS^{G12V} or HRAS^{G12V}-MYC expressing HTK1-E6E7 cells. HTK1-E6E7-HRAS^{G12V} cells showed the fastest growth rate. Cells were grown as described in (B). (**F**) Anchorage independent growth of HTK1-E6E7 cells expressing different transgenes performed as for (C). Scale bars, 250 μm.

(**Figure 2F**). HTK1-E6E7- HRAS^{G12V} cells (3/4) as well as HTK1-E6E7- HRAS^{G12V}-MYC cells formed tumors (8/8) in nude mice, whereas those expressing MYC alone failed to do so (**Table 1**). This is consistent with our previous results that a combination of E6E7 and oncogenic HRAS without MYC can confer tumorigenicity on human cervical keratinocytes and MYC substantially enhances the tumorigenicity. These results indicate that a combination of oncogenic HRAS and MYC can cooperately confer anchorage-independent growth and tumorigenicity on HTK cells expressing either E6E7 or CDK4/cyclin D1/TERT and DNp53.

Combined transduction of a constitutively active form of EGFR and a degradation-resistant form of MYC into HTK1-K4DT-DNp53 and HTK1-E6E7 cells induces anchorage-independent growth and tumor-forming ability in nude mice

Excluding cases in tobacco chewers, overexpression of EGFR or activating mutations of EGFR are observed more frequently than activating mutations in the RAS oncogenes [17, 35]. To determine a role of enhanced EGFR signaling in the development of OSCCs, wild type EGFR (EGFR^{WT}) or a constitutively active form of EGFR (EGFR$^{d746-750}$) instead of HRAS was transduced into HTK1-K4DT and HTK1-E6E7 cells as expected if HRAS and EGFR are acting in the same pathway. Expression of the transgenes was confirmed by immunoblotting (**Figure 3A** in HTK1-K4DT and **Figure 4A** in HTK1-E6E7). Total and the phosphorylated form of EGFR in HTK1-K4DT-DNp53-EGFR^{WT} cells and HSC2

Table 1. Summary of data for tumorigenic potential of HTK1 and HTK3 cells with various transgenes (1×106 cells/site).

Cells		No. of tumors/ Sites of injection	Cells	No. of tumors/ Sites of injection
HTK1-K4DT-DNp53-HRAS^{G12V}			HTK3-K4DT-DNp53-HRAS^{G12V}	
vector	exp 1	0/4	vector	0/4
	exp 2	0/4	MYC^{T58A}	4/4 (3)
MYC		4/4 (3)		
MYC^{T58A}		4/4 (4)		
HTK1K4DT-DNp53-EGFR^{WT}			HTK3-K4DT-DNp53-EGFR^{WT}	
vector		0/4	vector	0/4
MYC^{T58A}	exp 1	4/4 (7)	MYC^{T58A}	4/4 (9)
	exp 2	4/4 (10)		
HTK1-K4DT-DNp53-EGFR$^{d746-750}$			HTK3-K4DT-DNp53-EGFR$^{d746-750}$	
vector		0/4	vector	0/4
MYC^{T58A}		4/4 (6)	MYC^{T58A}	4/4 (4)
HTK1-K4DT-HRAS^{G12V}				
vector		0/4		
MYC		1/4 (5)		
HTK1-K4DT-DNp53-MYC		0/4		
HTK1-E6E7-HRAS^{G12V}			HTK3-T-E6E7-HRAS^{G12V}	
vector		3/4 (5)	vector	0/4
MYC	exp 1	4/4 (4)	MYC^{T58A}	4/4 (6)
	exp 2	4/4 (4)		
MYC^{T58A}		4/4 (4)		
HTK1-E6E7-EGFR^{WT}			HTK3-T-E6E7-EGFR^{WT}	
vector		0/4	vector	0/4
MYC		0/4	MYC^{T58A}	0/4
MYC^{T58A}		0/4		
HTK1-E6E7-EGFR$^{d746-750}$			HTK3-T-E6E7-EGFR$^{d746-750}$	
vector		0/4	vector	0/4
MYC^{T58A}		4/4 (10)	MYC^{T58A}	4/4 (9)
HTK1-E6E7-MYC		0/4		

Incidence of tumor formation within 16 weeks of observation period was scored. Number in parentheses indicates observation period (weeks) when mice were killed because of the faster growth of one or more tumors in the same mouse. Some cell lines were repeatedly established. exp 1, 1st experiment; exp 2, 2nd experiment.

(human OSCC cell line with EGFR amplification) cells were higher than those in vector transduced cells and the phophorylation levels were further increased by the addition of EGF. As expected, the phosphorylation levels of EGFR^{WT} in EGFR$^{d746-750}$ expressing cells were much higher without addition of EGF, indicating ligand-independent activation of the EGFR$^{d746-750}$ (**Figure 3A**, P-EGFR). Exogenous EGFR expression levels in HTK1-K4DT or HTK1-E6E7 cells were comparable to that of HSC2.

HTK1-K4DT cells expressing EGFR^{WT} or EGFR$^{d746-750}$ grew faster than those with an empty vector (**Figure 3B**), and additional transduction of MYC^{T58A} only slightly enhanced proliferation in culture (**Figure 3B**). HTK1-K4DT-DNp53 cells expressing EGFR^{WT} or EGFR$^{d746-750}$ exhibited anchorage-independent growth, enhanced by additional MYC^{T58A} transduction, whereas those with empty vector formed no colonies (**Figure 3C**). HTK1-K4DT-DNp53 cells expressing EGFR^{WT} or EGFR$^{d746-750}$ were able to form tumors only when MYC^{T58A} was co-expressed (**Table 1**) and those with EGFR$^{d746-750}$ formed tumors faster than those with EGFR^{WT} (**Table 1**).

HTK1-E6E7 cells expressing EGFR$^{d746-750}$ grew faster than those expressing EGFR^{WT} (**Figure**